Observation of Quantum Oscillations between a Josephson Phase Qubit and a Microscopic Resonator Using Fast Readout

K. B. Cooper,[1] Matthias Steffen,[1,2] R. McDermott,[1] R.W. Simmonds,[1] Seongshik Oh,[1] D. A. Hite,[1]
D. P. Pappas,[1] and John M. Martinis[1,*]

[1]*National Institute of Standards and Technology, 325 Broadway, Boulder, Colorado 80305, USA*
[2]*Center for Bits and Atoms, MIT, Cambridge, Massachusetts 02139, USA*
(Received 27 May 2004; published 25 October 2004)

We have detected coherent quantum oscillations between Josephson phase qubits and critical-current fluctuators by implementing a new state readout technique that is an order of magnitude faster than previous methods. These results reveal a new aspect of the quantum behavior of Josephson junctions, and they demonstrate the means to measure two-qubit interactions in the time domain. The junction-fluctuator interaction also points to a possible mechanism for decoherence and reduced fidelity in superconducting qubits.

Superconducting circuits based on Josephson tunnel junctions have attracted renewed attention because of their potential use as quantum bits (qubits) in a quantum computer. Rapid progress toward this goal is indicated by the observation of Rabi oscillations in charge, flux, phase, and hybrid charge-flux based Josephson qubits [1–4]. In addition, coupled-qubit interactions have been inferred spectroscopically [5,6], and a two-qubit quantum gate has been implemented [7]. However, the direct detection of time-domain correlations in coupled qubits remains elusive. One obstacle to observing two-qubit dynamics is that the single-shot state readout time must be much shorter than the qubit coherence time (~ 10–100 ns) and the time scale of the coupled-qubit interaction. Fast readout techniques are also needed for error correction algorithms [8].

Here we report a high-fidelity state measurement of the phase qubit with a duration of only 2–4 ns. Using this new readout technique, we directly detect time-domain quantum oscillations between the qubit and the recently discovered spurious resonators associated with critical-current fluctuators in Josephson tunnel junctions [9]. These results explicitly illustrate the mechanism by which critical-current fluctuators decohere phase qubits. We also present a model that attributes reduced measurement fidelity to the spurious resonators, and speculate that qubit-fluctuator coupling contributes to decoherence and loss of fidelity in the flux and charge-flux qubits. In addition to revealing these new aspects of qubit physics, the few-nanosecond measurement technique will be valuable for future experiments on coupled qubits.

The design of Josephson phase qubits has been described previously [1,9], and Fig. 1(a) shows the principal circuitry used in this experiment. The qubit's Josephson junction is embedded in a superconducting loop, and current biasing of the junction is achieved by coupling flux into the loop from the nearby bias line. The bias current $I_\phi = I_{dc} + \delta I(t)$ consists of a slowly varying component I_{dc} and a short pulse $\delta I(t)$ used for the fast measurement scheme. Microwave currents $I_{\mu w}$, used to control the state of the qubit, are capacitively coupled to the qubit after passing through low-temperature attenuators (not shown). The dashed box in Fig. 1(a) surrounds on-chip components kept near 25 mK. Figure 1(b) shows the potential energy landscape of the qubit's Josephson phase, including the cubic confinement potential on the left that is characteristic of all Josephson phase qubits. The states labeled $|0\rangle$ and $|1\rangle$, separated by an energy $\hbar\omega_{10}$, are the two qubit states. Both $\hbar\omega_{10}$ and the depth of the left-hand well, ΔU, can be adjusted by varying I_ϕ.

Rabi oscillations between states $|0\rangle$ and $|1\rangle$ can be observed by irradiating the qubit with microwaves at a frequency $\omega/2\pi \approx \omega_{10}/2\pi \sim 5$–$10$ GHz and then measuring the qubit's probability of being in state $|1\rangle$. This
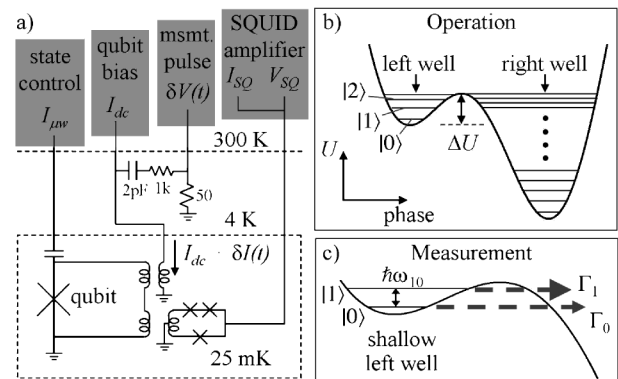

FIG. 1. (a) Schematic of the qubit circuitry, with Josephson junctions denoted by the symbol $\times$. For the qubit used in Fig. 2, the Josephson critical-current and junction capacitance are $I_0 \approx 10\ \mu$A and $C \approx 2$ pF; in Figs. 3 and 4, each of these values is about 5 times smaller. (b) Potential energy landscape and quantized energy levels for $I_\phi = I_{dc}$ prior to the state measurement. (c) At the peak of $\delta I(t)$, the qubit well is much shallower and state $|1\rangle$ rapidly tunnels to the right-hand well.

probability was previously measured by applying microwaves at a frequency ω_{31} for a duration of 80–100 ns. If the qubit is initially in state $|1\rangle$, the ω_{31} signal causes a transition to state $|3\rangle$, quickly followed by the qubit tunneling into the right-hand well. In this way, the qubit measurement consists of mapping the states $|0\rangle$ and $|1\rangle$ into the left and right-hand wells, which are separated by a single flux quantum in the qubit loop. At a later time, the result of this measurement can be learned by acquiring the I-V curve of a SQUID amplifier positioned to detect flux changes in the qubit loop. We emphasize that the qubit state measurement time (i.e., the time required to induce conditional tunneling out of the left-hand well) is *independent* of the SQUID amplification step. Also, by using the $1 \rightarrow 3$ transition tunneling scheme, the measurement time cannot be made significantly shorter than ~80 ns because of the need to balance the strength of the transition against the tunneling rate of state $|3\rangle$.

Here, a faster state measurement is achieved by applying a short bias current pulse $\delta I(t)$ that adiabatically reduces the well depth $\Delta U/\hbar\omega_p$ so that the state $|1\rangle$ lies very near the top of the well when the current pulse is at its maximum δI_{max} [see Fig. 1(c)]. The value of δI_{max} is chosen so that the tunneling rate Γ_1 of state $|1\rangle$ at δI_{max} is high enough for $|1\rangle$ to tunnel during the application of $\delta I(t)$. Also, because Γ_1 is at least 2 orders of magnitude larger than the tunneling rate Γ_0 of $|0\rangle$, a single current pulse yields a reliable measurement of the probability that $|1\rangle$ is occupied. Calculations suggest that the ratio of tunneling rates for shallow wells is $\alpha = \Gamma_1/\Gamma_0 \approx 150$, and that the corresponding maximum measurement fidelity is $\eta \approx 0.96$. Here η is defined as the difference of the tunneling probability when the qubit state is in state $|1\rangle$ versus state $|0\rangle$.

The fast-pulse $\delta I(t)$ is generated by capacitively coupling a voltage step $\delta V(t)$ to the qubit bias line [see Fig. 1(a)]. Room temperature measurements reveal that $\delta I(t)$ has a width of about 5 ns, as shown in Fig. 2(a). This is sufficiently slow to maintain adiabaticity with respect to the subnanosecond time scales of intrawell transitions. The actual measurement time is somewhat shorter than the full width of $\delta I(t)$ because the tunneling rate Γ_1 is *exponentially* sensitive to the total bias current I_ϕ. Therefore, the qubit will be far more likely to tunnel near the peak of $\delta I(t)$ rather than its flanks, including the long trailing edge of $\delta I(t)$ arising from impedance mismatches in the current bias line. We estimate the effective measurement duration to be 2–4 ns. This is more than an order of magnitude shorter than the microwave measurement technique as well as the readout methods used in most other superconducting qubits [10].

The data in Fig. 2(b) demonstrate the effectiveness of the fast measurement scheme. The solid circles are the tunneling probability of the qubit as a function of the pulse height δI_{max} when no radiation at ω_{10} is applied, i.e., when the qubit is in state $|0\rangle$. The data were obtained at an
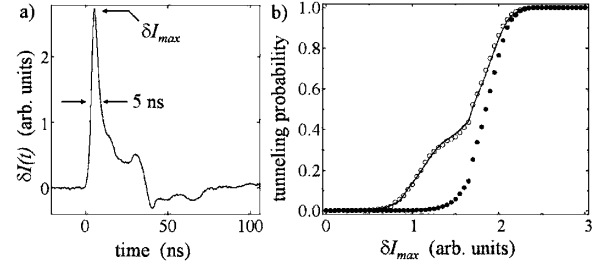

FIG. 2. (a) Room temperature measurement of the fast current pulse. (b) Tunneling probability versus δI_{max} with the qubit in state $|0\rangle$ (solid circles) and in an equal mixture of states $|1\rangle$ and $|0\rangle$ (open circles). Fit to data is shown by the solid line. The plateau, being less than 0.5, corresponds to a maximum measurement fidelity of 0.63.

initial well depth of $\Delta U = 4.5\hbar\omega_p$, where $\omega_p \approx \omega_{10}/0.9$ is the classical plasma frequency of the Josephson junction. The open circles in Fig. 2 are the measured tunneling probabilities as a function of δI_{max} after a microwave drive at ω_{10} saturates the populations of $|0\rangle$ and $|1\rangle$ approximately equally. To produce a nearly 50/50 mixture of $|0\rangle$ and $|1\rangle$, microwaves were applied for 500 ns, much longer than the qubit's T_1 time, and their power was high enough that the Rabi oscillation period of about 10 ns is shorter than T_1. The plateau in the tunneling probability data occurs around the values of δI_{max} where state $|1\rangle$ has a high tunneling rate while state $|0\rangle$ remains mostly confined in its potential well. For equal populations of $|0\rangle$ and $|1\rangle$, the plateau should level out near 0.50 for the predicted measurement fidelity of $\eta = 0.96$. Instead, the measured tunneling probability plateaus around 0.35, suggesting a slightly lower fidelity. Indeed, fitting the data to a simple model [solid line in Fig. 2(b)] yields a maximum fidelity of $\eta = 0.63$. This curve fit was made by finding the best weighted average of the tunneling probabilities for states $|0\rangle$ and $|1\rangle$. The former probabilities are the solid points in Fig. 2(b), while the latter are taken to be those same points shifted to the left by an amount that gives the best fit.

The new state readout scheme is capable of measuring the spectroscopy of the $0 \rightarrow 1$ transition for a broad range of well depths, as shown in Fig. 3. The data were obtained from a qubit with a slightly lower fidelity ($\eta \approx 0.5$) than that of Fig. 2(b), but both exhibit the same essential behavior. The gray scale is proportional to the occupation probability at state $|1\rangle$ after a long, low-power microwave drive is applied and δI_{max} is adjusted to optimize the signal at each flux bias point. Figure 3 shows a series of resonance splittings that likely arise from an interaction of the qubit with individual critical-current fluctuators at microwave frequencies [9]. Treating a single fluctuator as two-level quantum systems and labeling its ground and excited states as $|g\rangle$ and $|e\rangle$, a coupling of strength $hS/2$ will split the direct-product states $|1g\rangle$ and $|0e\rangle$ by hS when the qubit energy $\hbar\omega_{10}$ is tuned to the fluctuator

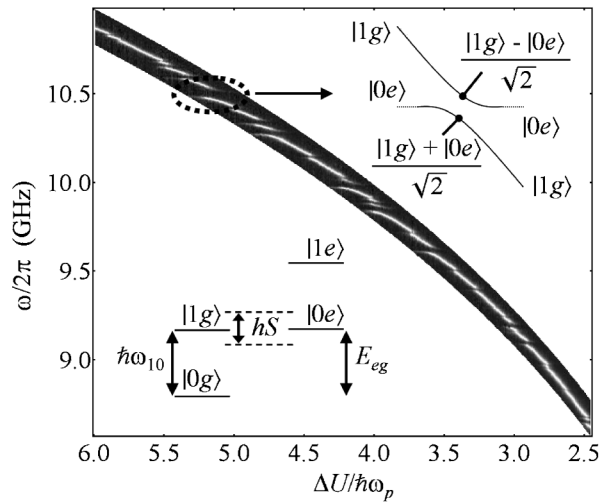FIG. 3. Spectroscopy of ω_{10} obtained using the current-pulse measurement method as a function of well depth $\Delta U/\hbar\omega_p$. For each $\Delta U/\hbar\omega_p$, the gray scale intensity is the normalized tunneling probability, with an original peak height of 0.1–0.3. Insets: A given splitting in the spectroscopy of magnitude S comes from a critical-current fluctuator coupled to the qubit with strength $hS/2$. On-resonance, the qubit-fluctuator eigenstates are linear combinations of the states $|1g\rangle$ and $|0e\rangle$, where $|g\rangle$ and $|e\rangle$ are the fluctuator states.
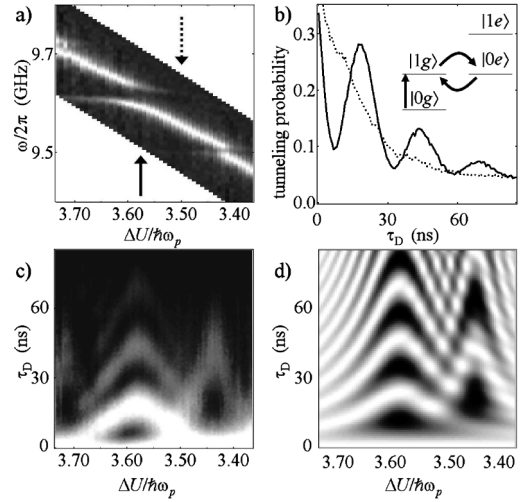

FIG. 4. (a) Detail of the qubit spectroscopy near $\Delta U/\hbar\omega_p = 3.55$, showing splittings of strengths $S \approx 44$ and 24 MHz. (b) Tunneling probability versus measurement delay time τ_D after application of π pulse. Solid (dashed) line is taken at a well depth of solid (dashed) arrow in (a), corresponding to a resonant (off-resonant) bias. The inset illustrates how the qubit probability amplitude first moves to state $|1g\rangle$ and then oscillates between $|1g\rangle$ and $|0e\rangle$. (c) and (d) Tunneling probability (gray scale) versus well depth and τ_D for experimental data (c) and numerical simulation (d). The peak oscillation periods are observed to correspond to the spectroscopic splittings.

energy E_{eg} (see insets to Fig. 3). Splittings as large as $S \approx 70$ MHz are visible in Fig. 3.

Simmonds *et al.* have already shown that the qubit's Rabi oscillations have reduced coherence when ω_{10} is tuned near a splitting in the spectroscopy [9]. To better understand the spurious resonators' effect on the qubit, it is helpful to examine the *dynamics* of the qubit-fluctuator interaction directly, and the few-nanosecond readout method allows us to accomplish this. Figure 4(a) shows a section of the spectroscopy of Fig. 3 around $\Delta U/\hbar\omega_p = 3.6$, where a strong, well-isolated splitting occurs at $\omega_{10}/2\pi = 9.62$ GHz with a magnitude of $S \approx 44$ MHz. A smaller splitting of magnitude $S \approx 24$ MHz is visible at a slightly shallower well depth. Figure 4(b) shows the time-domain response of the qubit to an 8 ns π pulse for the qubit tuned to the center (solid) and away from (dashed) the 44 MHz splitting in Fig. 4(a). Following the π pulse, the fast measurement probe is applied after a delay of τ_D to measure how the occupation probability of $|1\rangle$ changes with time. For a well depth $\Delta U/\hbar\omega_p = 3.50$, the dashed curve in Fig. 4(b) exhibits an exponential decay with a time constant that is roughly $T_1 \approx 25$ ns [11]. In contrast, the solid curve in Fig. 4(b) shows that when the qubit is tuned to a large splitting, at $\Delta U/\hbar\omega_p = 3.58$, a striking oscillation in the tunneling probability is superimposed on the T_1 decay curve. Note that this is *not* a Rabi oscillation because there is no microwave driving power at ω_{10}. Instead, its period of 24 ns is very close to the inverse of the measured splitting size $S^{-1} = 23$ ns, which is expected from the model of the qubit coupled to

a critical-current fluctuator with a strength $S/2$. As shown in the inset to Fig. 4(b), after the qubit is promoted to state $|1g\rangle$ by the π pulse, the qubit-fluctuator interaction will cause an oscillation between $|1g\rangle$ and $|0e\rangle$ at a frequency S as energy is transferred back and forth between the qubit and the fluctuator. The data in Fig. 4 thus constitute compelling evidence for coherent quantum oscillations between the mesoscopic qubit and a single microscopic fluctuator.

A further test of this model is to track the time-domain response of the qubit over a narrow range of bias currents around the fluctuator's resonant frequency. As the qubit bias is moved away from the major resonance near $\Delta U/\hbar\omega_p = 3.60$, Fig. 4(c) shows that the oscillation frequency increases as the states $|1g\rangle$ and $|0e\rangle$ become nondegenerate. An interaction between the qubit and a smaller splitting near $\Delta U/\hbar\omega_p = 3.41$ is also evident. Remarkably good agreement with this data comes from the simulation shown in Fig. 4(d). The simulation, where dissipation is ignored, is obtained by numerically integrating the Schrödinger equation for the three-level subspace of $|1g_1 g_2\rangle$, $|0e_1 g_2\rangle$, and $|0g_1 e_2\rangle$. The three levels denote the product states of the qubit with fluctuator states $|g_i\rangle$, $|e_i\rangle$, for $i = 1, 2$, corresponding to the large and small splittings of Fig. 4(a). The coupling strengths between the three states were chosen to match the observed splitting sizes. While these results are consistent with the fluctuators being strictly two-level systems, our simulations and experimental results do not rule out the

possibility that a given fluctuator might have other excited levels out of resonance with the qubit. We emphasize that these results could not have been obtained using the previous microwave measurement method because the signals would be averaged out over the ~100 ns measurement time. Also, the demonstration of dynamical coupling between the qubit and a critical-current fluctuator suggests that we now have the tools to successfully measure the coupling between two Josephson phase qubits.

Interestingly, the data of Fig. 4 suggest that the coherence time of a critical-current fluctuator can be at least as long as that of the qubit. After all, once the fluctuator absorbs the qubit energy after ~10 ns, it does not immediately decay from $|0e\rangle$ to $|0g\rangle$. In fact, the decay envelope of the on-resonance signal in Fig. 4(b) is about 1 to 2 times the T_1 of the qubit away from a large resonator, indicating that the decay time of a strong critical-current fluctuator is at least as long as the qubit's T_1 time. We thus speculate that spin-echo techniques might be able to refocus some of the signal lost to spurious resonators [12]. Another unexplored feature of the qubit-fluctuator interaction is the effect of small fluctuators not resolved in the spectroscopy data. Analyses of the resonator distributions could reveal how strongly such an ensemble of coupled critical-current fluctuators would affect the qubit and whether this might be a factor in the short T_1 observed.

Another consequence of the dynamic qubit-resonator interaction is reduced fidelity of the fast-pulse measurement. As $\delta I(t)$ increase during a measurement, the qubit moves in and out of resonance with many spurious resonators before any tunneling occurs. If the qubit is initialized in state $|1\rangle$, then each resonator absorbs a small amount of the $|1\rangle$ probability amplitude during the measurement pulse, leaving the qubit with some amplitude in state $|0\rangle$. The probability of remaining in state $|1\rangle$ after sweeping through a single fluctuator of strength $hS/2$ can be estimated from the Zener-Landau tunneling formula $P(S) = \exp(-\pi^2 S^2/\dot{f}_{10})$, where $\dot{f}_{10} = \dot{\omega}_{10}/2\pi$ is the rate of change of the qubit frequency during the sweep [13].

Accounting for the effect of a collection of N_{S_i} resonators of splitting size S_i, the total measurement fidelity becomes $\eta \approx \Pi_i P(S_i)^{N_{S_i}}$. For the qubit used in Fig. 2, spectroscopic measurements indicate that the rms splitting size of the 45 visible splittings is $S_{\text{rms}} \approx 30$ MHz. Assuming the $\delta I(t)$ results in a frequency sweep rate of $\dot{f}_{10} \approx 1$ GHz/ns, we find that the measurement fidelity would be reduced from $\eta \approx 1$ to $\eta \approx 0.7$. The actual fidelity of the qubit of Fig. 2 is $\eta = 0.63$, and therefore the qubit-fluctuator interaction is likely a prominent source of fidelity loss in the fast-pulse measurement method. Surprisingly, the Landau-Zener model predicts that the fidelity should become *worse* as the measurement duration becomes *longer*. Preliminary experiments involving slower pulses of $\delta I(t)$ are consistent with this prediction, but separating the effect of fidelity loss from the

signal loss is difficult because of the short T_1 times. Nonetheless, this effect may be relevant to the flux and the charge-flux qubits [3,4] where fidelities of $\eta \sim 0.6$ have been observed, and where similar current-pulse schemes for state measurement and manipulation are used. However, in the case of the charge qubit a probability plateau analogous to that of Fig. 2(b) is absent, and the fidelity is estimated indirectly from the amplitude of Rabi oscillations [14]. Whether these lowered fidelities can be attributed to microscopic fluctuators remains to be investigated.

In conclusion, we have implemented a state measurement technique for the Josephson phase qubit that is an order of magnitude faster than the microwave measurement method. With a temporal resolution of less than 5 ns, the fast-pulse method reveals coherent quantum oscillations between the qubit and a microscopic resonator embedded within the qubit circuit. The dynamics of the qubit-resonator interaction illustrate one mechanism by which the coherence of a superconducting qubit is lost to its environment. The size and number of the resonators suggest that they are relevant to fidelity loss in pulse measurements, and we predict that the fidelity should increase as the measurement duration decreases. These results underscore the importance of understanding the details of Josephson junction physics in order to explain the quantum behavior of superconducting qubits. They also prove that the tools are available for a time-domain demonstration of the coupling of two phase qubits.

---

*Electronic address: martinis@physics.ucsb.edu
[1] J. M. Martinis, S. Nam, J. Aumentado, and C. Urbina, Phys. Rev. Lett. **89**, 117901 (2002).
[2] Y. Nakamura, Y. A. Pashkin, and J. S. Tsai, Nature (London) **398**, 786 (1999).
[3] I. Chiorescu, Y. Nakamura, C. J. P. Harmans, and J. E. Mooij, Science **299**, 1869 (2003).
[4] D. Vion et al., Science **296**, 886 (2002).
[5] A. J. Berkley et al., Science **300**, 1548 (2003).
[6] Y. A. Pashkin et al., Nature (London) **421** , 823 (2003).
[7] T. Yamamoto et al., Nature (London) **425**, 941 (2003).
[8] D. P. DiVincenzo, Fortschr. Phys. **48**, 771 (2000).
[9] R. W. Simmonds et al., Phys. Rev. Lett. **93**, 077003 (2004).
[10] Very recently, fast (2−5 ns) state measurements were reported in flux qubits and in a dc-SQUID circuit. See P. Bertet et al., Phys. Rev. B **70**, 100501 (2004); J. Claudon et al., cond-mat/0405430 [Phys. Rev. Lett. (to be published)].
[11] The expected T1 times are on the order of microseconds, and the cause of the fast energy relaxation is under investigation.
[12] N. Linden, H. Barjat, R. J. Carbajo, and R. Freeman, Chem. Phys. Lett. **305**, 28 (1999).
[13] C. Zener, Proc. R. Soc. London A **137**, 696 (1932).
[14] D. Vion (private communication).